PNAS Nexus, 2024, 3, pgae129
https://doi.org/10.1093/pnasnexus/pgae129
Advance access publication 16 April 2024
Research Report

Existing wetland conservation programs miss nutrient reduction targets

Shan Zuidema [a,*], Wilfred M. Wollheim [a,b], Christopher J. Kucharik [c] and Richard B. Lammers [a]

[a]Earth Systems Research Center, University of New Hampshire, Durham, NH 03824, USA
[b]Department of Natural Resources, University of New Hampshire, Durham, NH 03824, USA
[c]Department of Plant and Agroecosystem Sciences, University of Wisconsin-Madison, Madison, WI 53706, USA
*To whom correspondence should be addressed: Email: shan.zuidema@unh.edu
Edited By: Barbara Romanowicz

Abstract

Restoring wetlands will reduce nitrogen contamination from excess fertilization but estimates of the efficacy of the strategy vary widely. The intervention is often described as effective for reducing nitrogen export from watersheds to mediate bottom-level hypoxia threatening marine ecosystems. Other research points to the necessity of applying a suite of interventions, including wetland restoration to mitigate meaningful quantities of nitrogen export. Here, we use process-based physical modeling to evaluate the effects of two hypothetical, but plausible large-scale wetland restoration programs intended to reduce nutrient export to the Gulf of Mexico. We show that full adoption of the two programs currently in place can meet as little as 10% to as much as 60% of nutrient reduction targets to reduce the Gulf of Mexico dead zone. These reductions are lower than prior estimates for three reasons. First, net storage of leachate in the subsurface precludes interception and thereby dampens the percent decline in nitrogen export caused by the policy. Unlike previous studies, we first constrained riverine fluxes to match observed fluxes throughout the basin. Second, the locations of many restorable lands are geographically disconnected from heavily fertilized croplands, limiting interception of runoff. Third, daily resolution of the model simulations captured the seasonal and stormflow dynamics that inhibit wetland nutrient removal because peak wetland effectiveness does not coincide with the timing of nutrient inputs. To improve the health of the Gulf of Mexico efforts to eliminate excess nutrient, loading should be implemented beyond the field-margin wetland strategies investigated here.

Keywords: wetland restoration, nitrogen, hypoxia, modeling

Significance Statement

The range in the amount of nitrogen potentially reduced by restoring wetlands across the Mississippi River Basin is explained by considering more realistic constraints on restoration. By considering new estimates of the locations where wetland restoration could occur, estimates of flow to groundwater from croplands, and differences in the seasonal timing of nitrogen removal activity in wetlands we estimate that export to the coast could decline by 6 to 27% compared to the 45 to 60% needed to support the marine ecosystem. The moderate levels of nitrogen reduction provide a range of best-case scenarios suggesting that a collection of interventions is needed to adequately solve the crisis of nutrient loading to our coasts.

Introduction

Increasing coastal hypoxia results largely from riverine export of excess nutrients used for fertilization of row crops (1–4) and has the potential to fundamentally change marine habitats over the next millennium (5). Multiple models and methods show that the nutrient content in runoff from agricultural lands in the Mississippi/Atchafalaya River Basin must decline by half to begin reducing hypoxia in the Gulf of Mexico (6, 7). While comprehensive management studies weigh the benefits of nutrient mitigation using multiple strategies and targeting hot spots of excess fertilizer application or manure production (8, 9), numerous studies identify wetland restoration as important to achieving the needed nutrient reduction targets (10–15).

To mitigate coastal hypoxia, field-margin interventions that intercept nitrogen-laden water between crop fields and streams, including in situ bioreactors (16, 17), riparian infiltration (18), and constructed wetlands are often cited as effective nutrient reduction strategies (19–23) as they exhibit high nutrient removal capacity, require low-to-moderate operational labor, and have numerous synergistic benefits such as carbon sequestration (24) and habitat building (25). Recent studies at continental scales to predict restoration effects show divergent estimates of nitrate

Competing Interest: The authors declare no competing interest.
Received: September 13, 2023. **Accepted:** March 14, 2024

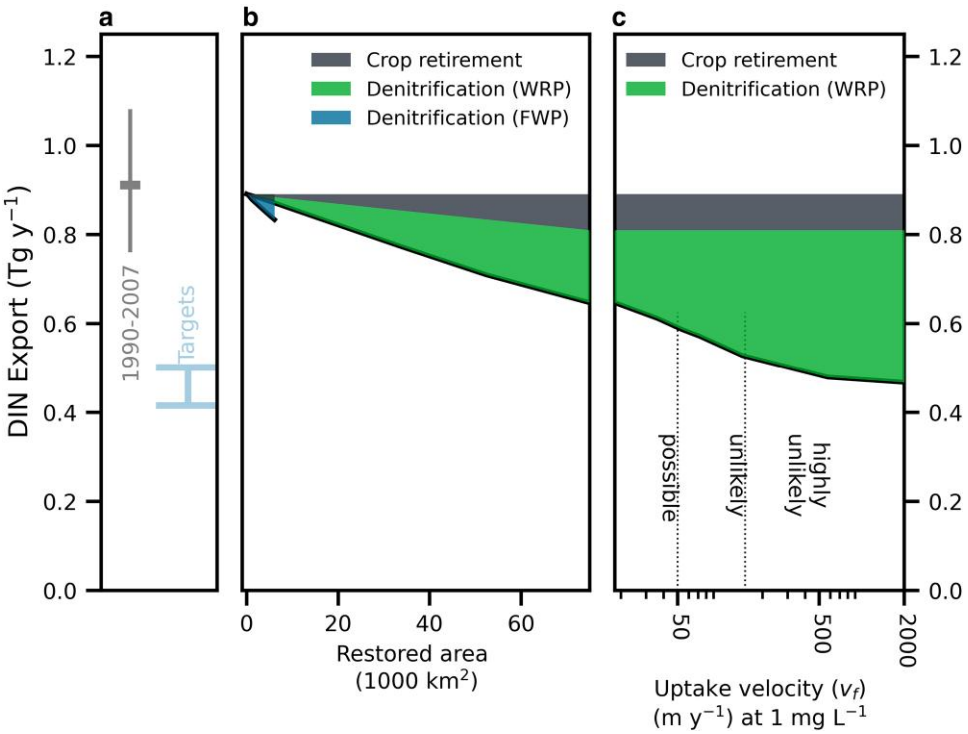

Fig. 1. Nitrate export from the MRB. a) present day accounting for interannual variability with established targets, b) following adoption of two wetland restoration programs attributable to reduced leaching as croplands are converted to wetlands, and denitrification within restored wetlands. Maximum area of restoration in the FWP and the Wetland Reserve Program are 6,000 and 70,000 km^2, respectively. Prior studies of wetland restoration predict generally greater reductions in nitrate (numbers indicate study references). c) Sensitivity of additional export reduction in the WRP to a range of enhanced wetland denitrification rates encompassing values previously reported for natural or restored wetlands to illustrate the physical limit of wetland restoration to reduce nitrate export. Values of the uptake velocity v_f at 1 mg NO_3-N L^{-1} and 20 °C up to 400 m y^{-1} have been observed in nature.

reduction in riverine exports from the Mississippi ranging from 1.6% (8) to 54% (19). Several factors may explain the differences among prior estimates of wetland removal. The position of wetlands in the landscape (22, 26) constrain the amount of leachate a wetland may intercept. The distribution of transport timescales (27–29) affects the efficiencies of these systems to remove nutrients through denitrification, which can create pulses of increased nitrate flux from wetlands to receiving waters especially during high input storms (30, 31) and when water temperature is cool (29). Finally, nitrogen lost from soil takes numerous flow paths, including storage within long-term pools contributing to legacy nitrogen storage (32, 33), which may preclude access by restored wetlands for denitrification. Properly evaluating the influence of these factors on projected nitrogen removal by wetlands requires a whole-system approach.

Engineering considerations further constrain how and where restoration can be most effective. Wetlands can be restored or constructed to intercept agricultural runoff from a variety of flow paths (23, 34). Engineering constraints such as catchment size and buffer width surrounding active wetlands protect the systems but limit how much runoff wetlands can process (21, 23). Wetlands affect hydrologic response in streams (35), with floodplain wetlands connected to rivers further downstream permitting greater interception of nutrients maximizing denitrification potential (19, 22, 26). Subsurface drains (SSDs) are widely distributed throughout the mid-western United States (36, 37), and leachate from corn/soy rotations grown on SSD croplands represent the largest single source of excess nitrogen discharged to the Gulf of Mexico (3). Restoration of lands that neglect leachate from SSD may have modest effects on nitrate reduction at the watershed scale (38). Despite the above complexities denitrified mass fractions in individual wetlands often fall within a range of 40 to 50% removal of input nitrate, so many macroscale studies assume homogenous response to wetland restoration (8, 13, 20, 21). But such approaches neglect dynamic hydrology and seasonal effects and often neglect wetland placement relative to sources.

Fully process-based models of coupled land–water ecosystems, like the ones used here, are required to scale estimates of wetland denitrification and consider the constraints on wetland restoration imposed by climate, geography, operations, and existing policies facilitating adoption of this intervention. We evaluate the efficacy of plausible wetland restoration on identified restorable lands (39) across gradients of implementation. We used estimates of potential wetland extent based on their relative topographic position and ignored constraints from soil properties which maximizes potential restoration area. The modeled scenarios follow restoration strategies that reflect two federal programs in the United States (the Farmable Wetlands Program (23) and the Wetlands Reserve Program (40), FWP and WRP, respectively). In our model scenarios, the two programs differed based on upstream catchment area that is targeted for interception and subsurface drainage status of treated crops: FWP required large catchments of solely tile-drained crops (23); WRP included smaller catchments with no constraint on subsurface drainage status. Importantly, both programs assumed that catchments upstream of restored wetlands are completely cropped, which simultaneously maximizes delivery of nitrate runoff from crops to restored wetlands while minimizing crop retirement. In practice, it is unlikely that restored wetlands can be constructed to achieve complete interception of crop runoff, which biases estimated wetland efficacy toward greater removal for a given area restored and therefore represent an upper limit of each program's potential.

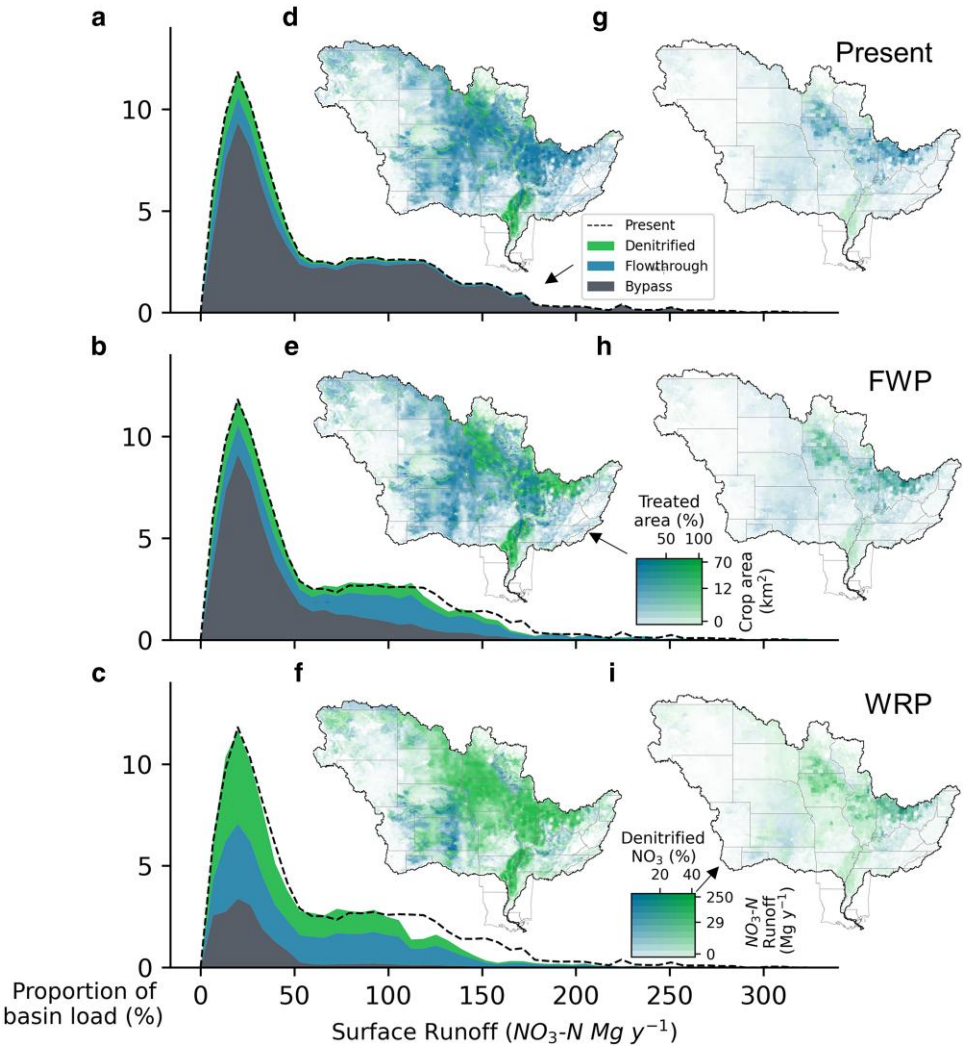

Fig. 2. The spatial distribution of present and restorable wetlands explains the amount and distribution of wetland nitrate removal. Distribution of nitrate fate prior to entering the river network as density plots for all pixels binned by nitrate flux in surface runoff (proportion) for a) present-day baseline, b) full adoption of the FWP, and c) the Wetland Reserve Program. Present-day total distribution of surface runoff repeated in b and c; white area below dashed line represents reduction in runoff from retiring crops to support restoration. d–f) Crop area maps for present-day and restored conditions presented as color intensity with fraction of that area treated by wetlands represented by color. g–i) Nitrate in surface runoff maps for present-day and restored conditions presented as color intensity with fraction of that runoff denitrified represented by color.

Our analysis used coupled models of agroecology (Agro-IBIS) (41–43) and hydrologic biogeochemistry (Water Balance Model, WBM) (44–46) (see Materials and methods). The models account for daily timescale dynamics of hydrologic flows and biologic nitrogen demand associated with season and storms, viable locations for wetland restoration, subsurface flow paths bypassing wetland treatment, and constraints on wetland inundation depth and buffer areas. Our results reflect inputs specified by policies or supported empirically, and model sensitivity testing reveals that our findings are robust across a broad range of conditions (see Materials and methods).

Results and discussion

We found that wetland restoration through existing federal programs incentivizing construction of field-margin wetlands could not reduce nitrate by the 45% (6) to 60% (7) needed to restore ecosystem health in the Gulf of Mexico (Fig. 1). At complete adoption restoration via the FWP and WRP could reduce nitrate export by 6.2 and 27%, respectively. These reductions occurred by increasing denitrification by 85 and 430% above that denitrified by the 45,000 km^2 of natural wetlands in the basin. Reduced nitrate leachate was responsible for approximately 29% (FWP) and 33% (WRP) of the simulated decline in nitrate export as croplands were retired to make room for restored wetlands and their buffers (Fig. 1). The high proportion of export reduction due to denitrification rather than crop retirement illustrates why wetland restoration is an ideal intervention for mitigating nutrient pollution in highly agricultural basins. We find that plausible restoration prescribed by the existing programs cannot achieve the needed nitrate reduction due to the geospatial separation of restorable wetlands with croplands, leaching to deeper flow paths that miss wetlands and reduced denitrification during storms and higher flows during colder temperature periods.

Geospatial separation constraints

Potentially restorable wetlands exist throughout the Mississippi River Basin (MRB); however, with the existing wetland restoration programs there remained sufficient geospatial separation between restorable areas and existing crops to limit the amount of

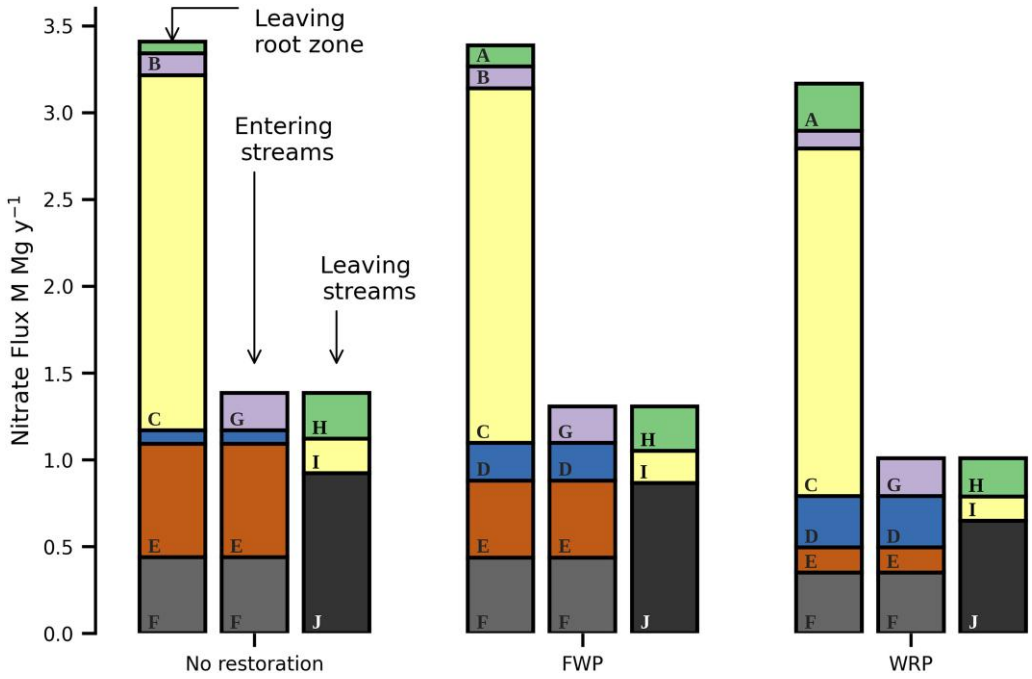

Fig. 3. Distribution of nitrate fluxes for present-day baseline, and complete adoption of the FWP, and Wetlands Reserve Program (WRP. Fluxes are separated by three stages of transport through the watershed and correspond to: A—denitrification within all wetlands, B—denitrification within shallow groundwater, C—storage or removal in other subsurface pools, D—flow out of wetlands to streams, E—flow bypassing wetlands to streams, F—baseflow nitrate from shallow groundwater to streams, G—other domestic inputs to streams from non-point source suburban development and waste water treatment plants, H—denitrification within streams, I—nitrate extraction from streams via water abstractions, and J—nitrate export to the Gulf of Mexico.

nitrate in surface runoff intercepted and treated. Bypassing flow in both programs was primarily a consequence of insufficient restorable wetlands (39) in regions containing target crops (Fig. 2). Catchment and buffer sizes explain most of the limitation of wetland interventions. Both programs assumed that 78% of restored cropland was reserved as buffer area without nitrogen removal potential, the complement was restored as active wetlands. Wetlands restored via full implementation of the WRP occupied 2.6% of their local catchments similar to natural wetlands (47), whereas FWP wetlands occupied 1% of their catchments (23).

The FWP program restored 6,000 km^2 of wetlands and buffers that intercepted runoff from 121,000 km^2 of crops. Of the 0.77 Tg y^{-1} of nitrate runoff from agricultural lands to streams, FWP wetlands intercepted 0.24 Tg y^{-1} (31%), while 52% of nitrate runoff bypassed both natural and restored wetlands (Fig. 2), and 16% was intercepted by natural wetlands. Nitrate flux in runoff from croplands and intercepted by restored wetlands via this program averaged 19.9 kg NO_3-N ha^{-1} y^{-1} (per crop area), and therefore, wetland denitrification exhibited denitrification rates of 313 kg NO_3-N ha^{-1} y^{-1} (per wetland area), consistent with observed values for treatment wetlands (48).

The WRP restored 70,000 km^2 of croplands that intercepted runoff from 498,000 km^2 of crops. WRP wetlands intercepted 0.45 Tg y^{-1} (70%) of agricultural nitrate, while 18% of agricultural nitrate bypassed wetlands and 12% was intercepted by natural wetlands (Fig. 2). Nitrate flux in runoff from croplands and intercepted by restored wetlands via this program was more modest than FWP, averaging 10.0 kg NO_3-N ha^{-1} y^{-1} (per crop area), resulting in wetland denitrification exhibiting lower areal denitrification 124 kg NO3-N ha^{-1} y^{-1} (per wetland area). While WRP had lower areal denitrification rates than FWP wetlands, they denitrified about 46% of the nitrate intercepted, compared to FWP wetlands that denitrified about 27% of intercepted nitrate (Fig. 2). Individual WRP wetlands removed a greater fraction of intercepted nitrate than FWP wetlands because catchments draining to them were smaller, leading to lower flow rates and more contact time with the wetland benthic surface, where most denitrification occurs. Furthermore, intercepted leachate in WRP was derived from a greater proportion of croplands leaching nitrate at lower rates compared to FWP which targeted heavily cropped areas with SSDs. Because we assumed nitrogen processing was inversely related to concentration (49) (see Materials and methods), wetland catchments with lower leaching intensity (WRP) exhibited higher proportional denitrification than those with higher leaching intensity (FWP). Nevertheless, restoration through the FWP removes more nitrate per area restored than WRP because greater denitrification will occur where more mass is treated. As the fraction of area that a wetland occupies inside its catchment increases the proportional removal of nitrogen increases, but the commensurate decrease in the mass treated necessarily exceeds any gains in efficiency of the denitrification reactions (see supplementary material).

Our analysis predicts greater nitrate removal by mass from wetland restoration than studies that limited restored areas by additional constraints than imposed here. Economic viability of restoration instruments from integrated assessment modeling predicted nitrogen reduction from field-margin wetland restoration to <2% (8, 11). Biophysical modeling, that assumed wetland restoration occurs only on nontile-drained land, limited nitrogen reduction to 12% (38).

Subsurface storage

The above reductions in nitrate export refer to changes from a present-day baseline condition that represents the major compartments and fluxes of nitrate in the terrestrial landscape

(Fig. 3). As such, deep subsurface storage is an important sink under present-day conditions. While this sink mitigates mass entering the subsurface, it also limits the absolute mass that restored wetlands can treat. The coupled models were able to achieve good correspondence with observed nitrate flux in rivers with parameterizations that removed much of the cropland leachate before entering wetlands or rivers (Figs. S1 and S2). Nitrate entering the subsurface is assumed to either enter a shallow groundwater pool experiencing denitrification at fixed rates (50) during transport toward streams, or percolates deeper in the subsurface to be stored (on net), or denitrified and considered to be removed from the surface water network for the duration of the model period. The fraction of total leachate calculated by Agro-IBIS percolating from the soil and stored deep in the subsurface needed to match river observations is the dominant flux in the simulations, equaling between 2.0 and 2.1 Tg y^{-1} of the 3.3 to 3.4 Tg y^{-1} leaching from the root zone (Fig. 3). Prior work identified the potential for net storage of this magnitude or greater in the root zone or below (3.5 Tg y^{-1} (32)), vadose zone or below (3.0 Tg y^{-1} (51)), or by increasing groundwater concentrations (2.6 Tg y^{-1} (52). A substantial fraction of such legacy storage in groundwater would be expected to discharge to rivers over long timescales, so the storage calibrated here is considered net storage (33, 53).

Previous studies of the potential for wetland restoration (19, 54) have found greater percent removal than we did when higher fractions of nitrate runoff (e.g. 30–50%) are assumed to be intercepted by wetlands. When we constrain the flux of agricultural runoff to deep groundwater stores using observed riverine nitrate flux, the highest fraction intercepted by restored wetlands was 16% for full adoption of the WRP (Fig. 3).

Temporal dynamics

Seasonality and storm-scale dynamics pose an additional constraint on nitrate removal by restored wetlands. The seasonal peak in wetland denitrification occurs in summer due to warmer temperatures when 41 and 62% of intercepted nitrate is removed from FWP and WRP wetlands, respectively. However, most influx to wetlands occurs during colder temperature periods (Fig. 4). The peak of the basin-average flux to restored wetlands occurred in May (representing 16% of total annual inputs to wetlands), when denitrification removed only 26% (FWP) and 39% (WRP) of intercepted nitrate due to colder temperatures. Storm bypass of nitrate due to flow depth exceeding specified maximums (55) was 6.9% (FWP) and 3.2% (WRP) of total annual nitrate runoff, mostly during the late winter and spring when soils are wetter and evapotranspiration is low (Fig. 4). A scenario where denitrification was independent of temperature indicates that seasonally colder temperatures reduce annual denitrification across the basin by 24% (Fig. 4d). Even if water does not bypass wetlands during storms, hydrological conditions are less favorable to denitrification. During periods of constant high runoff in spring, water depth was consistently higher within the wetlands, which increased hydraulic load and reduced contact between nitrate dissolved in the water column and the benthic surface thereby reducing denitrification (Fig. S3).

Internal wetland efficiency

When denitrification uptake approaches the highest rates observed in the literature, wetland removal efficiency increases sufficiently to meet coastal hypoxia targets (Fig. 1c). Baseline denitrification rates in WBM are conservative estimates

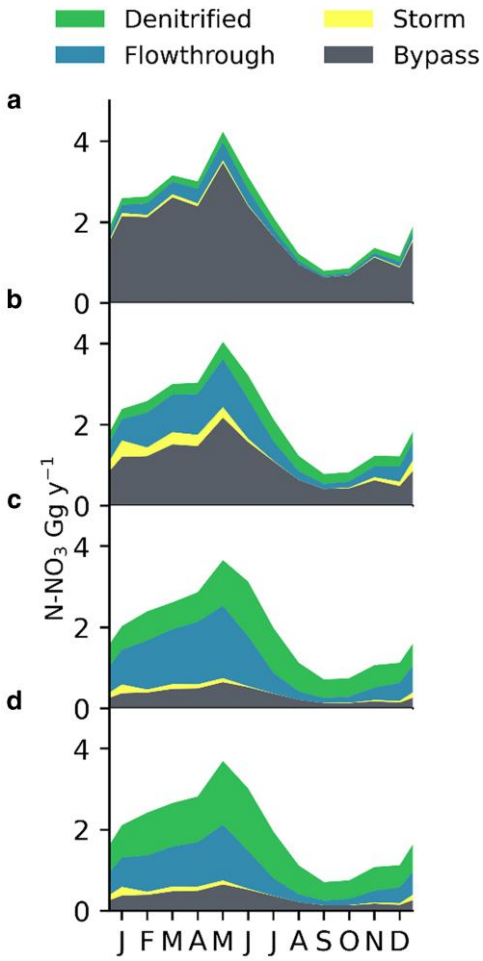

Fig. 4: Annual peak leachate flows precede seasonal wetland denitrification maximums. Monthly means of total basin fluxes for N runoff bypassing (not entering) wetlands, bypassing wetlands due to storms overwhelming wetland storage, entering wetlands but not denitrified (flowthrough) and denitrified in wetlands for a) present day with only unrestored wetlands, b) complete adoption of the FWP, c) complete adoption of the WRP, and d) complete adoption of the WRP assuming denitrification rates were unaffected by temperature. Sum of four fluxes represent total surface nitrate runoff from croplands. Storm bypass represents mass entering wetlands when water depth exceeded the maximum depth of 0.8 m and is modeled as entering rivers immediately.

consistent with rivers (56) and typical natural wetlands (54, 57); however, both natural and treatment wetlands have exhibited much higher rates in field studies (49, 58). Export reduction was highly sensitive to the parameter describing baseline denitrification rate (Figs.1c and S4). As denitrification rates approach an empirical maximum of about 400 m yr^{-1}, complete adoption of WRP was able to reduce nitrate export by 48%. However, assuming basin-scale average denitrification rates equal such high values is difficult to justify for the form of free-surface wetlands conceptualized in this analysis of the FWP or WRP.

Wetlands and groundwater

Characterizing the role of long-term storage and transformations of subsurface nitrogen, and to what degree it will be a long-term sink vs. source back to surface water, may be the single most important consideration defining the success of current nutrient reduction strategies (33, 59). Restored wetlands may be important in

treating nitrate from groundwater under a range of conditions not considered here. Lag times imposed by storage and travel through groundwater flow paths would be expected to evenly distribute mass input to wetlands throughout the year such that a high proportion could enter wetlands during summers when denitrification processes are most reactive.

Conclusion

While our study finds that existing field-margin wetland restoration programs can substantially contribute to N reduction to meet management goals, other management options, including other wetland restoration strategies, are necessary. Existing wetland policy programs investigated here assume direct connectivity to cropland runoff and can result in up to 60% of the required nutrient reduction needed to protect the Gulf of Mexico under ideal conditions. Restored fluvial wetlands, that exchange with river flows during downstream transport and potentially intercept groundwater and river flux from all upstream croplands, may be more effective at removing nitrogen than crop-margin wetlands at watershed scales (11). Policies should therefore include interventions that focus on fluvial wetlands (11) or floodplain restoration (60), while maintaining dialogue with stakeholders to address how conservation measures benefit and impact local communities and other ecosystem services provided by the watershed (61). As we consider the breadth of nature-based nutrient reduction strategies, we will need mechanistic evaluations of the role of temporal dynamics, position in the watershed, and future changes in both climate and cropping practices to ensure feasibility of these approaches. Field-margin wetlands are an important step toward mitigating Gulf of Mexico hypoxia because they have the capacity to reduce a meaningful fraction of nitrate and have existing conservation mechanisms in place to facilitate adoption.

Materials and methods

We coupled macroscale process models of agroecology (Agro-IBIS 41–43) and hydro-biogeochemistry (WBM 44–46) and introduced new functionality to WBM that represented water flow and nitrate transport from local croplands through field-margin treatment wetlands. Briefly, our model of wetland denitrification assumes a well-mixed system with denitrification occurring in benthic sediments parameterized as a temperature-dependent process ($Q_{10} = 2$), with flow and nitrate mass bypassing wetland processing when wetland water storage exceeds a maximum depth. The overall WBM framework applied here represents nitrate throughout the MRB considering remaining natural wetlands and scenarios of wetland restoration under the two national US programs that focus on highly optimized treatment wetlands on subsurface-drained crops (FWP (62)), and opportunistic restoration of wetland systems, where ecologically feasible (Wetland Reserve Program) (40).

Description of Agro-IBIS

Agro-IBIS is a processed-based, rasterized model of agroecology that calculates a suite of agronomic and ecological variables within the soil rooting zone (41–43). Agro-IBIS was run at a 5-arcminute resolution (66 ± 10 km^2) across the conterminous United States. Spin-up was performed from 1650 to 1947 to generate equilibrium soil biogeochemistry assuming appropriate vegetation cover throughout the epoch and recycling climate inputs from 1948 to 2007, then run from 1948 to 2007. Agro-IBIS calculates water and nutrient balance in the soil–plant–atmosphere system and calculates nitrate leaching below the root zone at 1.5 m (63). The model assumes all nitrate leaves the root zone via infiltration below the soil with no direct surface runoff. Agro-IBIS outputs pixel specific fluxes for each of 8 land-cover classes over agricultural areas of the MRB: (i) irrigated maize, (ii) rainfed maize, (iii) irrigated soy, (iv) rainfed soy, (v) irrigated soy/maize rotation, (vi) rainfed soy/maize rotation, (vii) rainfed wheat, and (viii) natural vegetation. The model has been previously corroborated against measures of nitrogen in harvest and leaching below the root zone (42, 43, 64, 65), primarily in the MRB.

Crop area

Nitrate leachate from Agro-IBIS was input to WBM following aggregation by crop area. Nitrate leachate flux at each pixel is that predicted for each crop type weighted by a representative area of each land cover. Crop cover fractions of each 5-arcminute pixel are aggregated and split between irrigated and rainfed crops using data representative of the year 2000 (66, 67). The total of irrigated and rainfed maize, soy, and wheat from these datasets represent 94% of all agricultural croplands in the MRB. Therefore, to complete our representation of row crop fluxes we define an "other crop" category, and associate other irrigated crops using nitrate fluxes calculated for irrigated maize, and other rainfed crops using an average of fluxes from rainfed maize and wheat.

To define the fraction of cropland undergoing annual maize/soy rotation, we calculate the fraction of 30-m pixels that transition from corn to soy or from soy to corn for each year of data (68) from 2008 to 2019, as well as those pixels that remain maize or remain soy for those years. We then aggregate to 5-arcminute resolution, to capture the relative fraction of continuously planted maize, continuously planted soy, and annual maize/soy rotation and assume these averages are appropriate for the year 2000.

Description of WBM

The University of New Hampshire WBM is a raster-based model of macroscale hydrology and biogeochemistry (44–46, 69), where previous model evaluation efforts were summarized in Ref. (46). We introduced new functionality to WBM that represented water flow and nitrate transport from local croplands through field-margin treatment wetlands (70) as described below. WBM was run at a 5-arcminute resolution over a geographic domain covering from 113°55′W (west) to 77°50′W (east), and 28°55′N (south) to 49°45′N (north). The evaluated domain covered the drainage basin of the Mississippi River defined by the MERIT 5-arcminute drainage network (71), and following postprocessing used to route drainage of small internally draining regions into the larger drainage network. WBM simulations were performed at a daily timestep. To perform model spin-up, needed only to equilibrate reservoirs, WBM was forced with input data from 1996 to 1999 repeated 5 times, then run from 1992 to 1997; a total of 26 years of model spin-up. We analyzed output data from 1998 to 2007. Description of model parameters used in the study and sensitivity of key model parameters are provided in Table S1. The representation of subsurface drainage in the model is also described in the supplementary material.

Representing wetlands in WBM

Field-margin wetlands are represented using a new pool within WBM that receives flow from upland portions of each pixel. For parsimony, the model combines riparian marginal processing, natural wetlands (where they still exist), and restored treatment

wetlands in a single pool. We acknowledge that engineering constraints imposed on wetland functionality presented are locally inappropriate for riparian areas and natural wetlands. Our formulation should conservatively estimate the amount of natural and riparian wetland denitrification that occurs because our assumptions of buffer area enforces an upper limit on the area that can be treated by present wetlands to smaller footprints than likely exist naturally (47). Furthermore, because we selected both moderate and highly probable potentially restorable wetlands, which reflected only topographic position constraints and not soil hydric potential constraints, we provide an upper limit on the estimate of restorable wetland areas feasible for at least the WRP scenarios. Parameter values controlling the wetland processes are described in the supplementary material.

The wetland pool occupies the lowest areas of each pixel along the riparian margin nearest streams such that it receives flow from surrounding uplands. This assumption maximizes the amount of crop runoff that can be treated and is consistent with the identification of potentially restorable wetlands (39). The water and nitrate mass balance of the wetland pool are governed by Eqs. 1 and 2, respectively:

$$\frac{dV}{dt} = I_{wl} - Q_{wl} \tag{1}$$

$$\frac{dM_{din}}{dt} = \dot{m}_{in} - \dot{m}_{den} - \dot{m}_{out} \tag{2}$$

Flow through the wetland pool is defined by both a maximum runoff defined by the area of upstream crop area draining into a wetland, and a maximum wetland depth (d_{max} [m]) which was selected as 0.8 m (55, 72). Time-varying flow from untreatable crops, and flow exceeding the maximum depth is routed immediately beyond the wetland to the stream (bypassing flow). Flow entering the wetland experiences a detention time specified by the wetland flow time-constant (α_{wl} [d^{-1}]) consistent with observations (73–75). These assumptions approximate dynamics in wetlands constructed for specific retention times and with overflow structures. The daily water balance is solved in three steps where bypassing flow is estimated (Eq. 3A), outflow is calculated assuming inflows from the midpoint of the timestep (Eq. 3B), and storage balance is updated (Eq. 3C):

$$I_{wl} = Q_{ro} \begin{cases} \frac{V_{avail}}{Q_{ro}dt} \; \frac{V_{avail}}{Q_{ro}dt} < \frac{\chi_{up}A_{wl}}{A_{crop}} \\ \frac{\chi_{up}A_{wl}}{A_{crop}} \; \frac{\chi_{up}A_{wl}}{A_{crop}} < \frac{V_{avail}}{Q_{ro}dt} \end{cases} \tag{3A}$$

$$Q_{wl} = (V^t_{wl} + I_{wl}\, dt\,)\alpha_{wl} \tag{3B}$$

$$V^{t+1}_{wl} = V^t_{wl} + I_{wl}\, dt - Q_{wl}\, dt \tag{3C}$$

This solution for wetland water balance accommodates WBM's source tracking functionality (46). The volume available (V_{avail}) within the wetland that results from flow depth below the specified maximum depth of flow (d_{max}) is calculated at each timestep (Eq. 4) and accounts for short-term storage over the duration of the timestep:

$$V_{avail} = (1 + \alpha_{wl}\, dt)A\ A_{wl}\ d_{max} - V_{wl} \tag{4}$$

The first term defines the maximum volume in the wetland, including volume released from the wetland during the timestep, and the second term represents the water volume existing in the waterbody at the beginning of the timestep.

Runoff from the upland portions of the pixel arrive to wetlands via quickflow in WBM to be consistent with design practice for treatment wetlands (55). Baseflow (flow from groundwater) is assumed to bypass wetlands and drain directly to streams. Our formulation for subsurface drainage routes through the quickflow flowpath in WBM (see supplementary material), which results in a majority of runoff from subsurface-drained agriculture entering wetlands where they are collocated in the same pixel. Although WBM assumes a single contiguous water surface and nitrate concentration for tractability, in practice multiple separate wetlands would be necessary to intercept leachate prior to loading to streams. Riparian marginal wetlands are included in our model to account for riparian uptake; a separate model treatment for such a process (76–78) was beyond the purpose of this study. The riparian marginal area (A_{wlR}) is parameterized as a fraction of the pixel calculated from an assumed buffer width (w_{wlR}) of 150 cm from stream margins (Eq. 5) that intercepts runoff prior to entering streams:

$$A_{wlR} = \frac{2\, L_{stream}\ w_{wlR}}{A} \tag{5}$$

The total wetland area is the sum of natural wetlands (A_{wlN}), introduced treatment wetlands (A_{wlT}), and riparian marginal wetlands. Riparian marginal wetlands exist only in the absence of natural or restored wetlands (Eq. 6):

$$A_{wl} = \min(A_{wlR},\ A_{wlN} + A_{wlT}) \tag{6}$$

A_{wl} represents the total wetland area, but a fraction (χ_{buffer}) of this total represents a buffer area that protects the wetland system. The complement fraction is the active water-holding wetland area (A_{wlA}) which holds water in storage and is where denitrification occurs. The active portion of wetlands (A_{wlA}) are assumed to have vertical banks (benthic area equals the active wetland area). The above assumptions lead to hydraulic loading in the active pool of simulated wetlands below 0.1 m d^{-1} where denitrification is most active (29).

Nitrate balance in wetlands is calculated with advective fluxes through the pool, and a denitrification flux within the pool. We assume that denitrification occurs in benthic sediments so that the process is parameterized with an uptake velocity v_f that is updated daily based on wetland nitrate concentration and temperature according to an efficiency loss parameterization (49) (Eq. 7):

$$v_f = \exp\left(\ln\left(b_{vf}\right) + a_{vf} \ln\left(C_{nitr}\right)\right) Q_{10}^{\frac{(T_{wl} - T_{ref})}{10}} \tag{7}$$

The relationship between v_f and concentration is a log-linear relationship in both lotic (56, 69) and lentic (49) systems, and is adjusted according to $Q_{10} = 2$ temperature reactivity (79), where water temperature is specified by Agro-IBIS at a depth of 1.5 m.

Nitrate balance within the wetlands is updated after calculating flow and water storage. Nitrate concentration (C_{nitr} [mg L^{-1}]) within the pool is updated at the midpoint of the timestep (Eq. 8A). The fractional removal of nitrate (R) from denitrification is calculated using an integral solution (Eq. 8B) (80), the mass flux denitrified and outflow are estimated (Eqs. 8C and 8D), and then total mass balance is updated (Eq. 8E):

$$C_{nitr} = (M^t_{nitr} + 0.5\dot{m}_{in}dt)/V^t_{wl} \tag{8A}$$

$$R = 1 - \exp\left(-\frac{v_f\ t}{d_{wl}}\right) \tag{8B}$$

$$\dot{m}_{den} = R\ \ (M^t_{nitr} + 0.5\ \dot{m}_{in}\ dt) \tag{8C}$$

$$\dot{m}_{out} = C_{nitr} Q_{wl} \quad (8D)$$

$$M_{nitr}^{t+1} = M_{nitr}^{t} + \dot{m}_{in}\,dt - \dot{m}_{den}\,dt - \dot{m}_{out}\,dt \quad (8E)$$

Mass flux is then routed to the stream network within the pixel. Comparable nitrogen dynamics are formulated within the stream system (44, 45).

WBM and Agro-IBIS do not presently have coupled soil water pools, so daily differences in percolation volume would introduce numerical instability between water volume and nitrate leachate mass. WBM exhibited flashier hydraulic response and greater retention of water within the soil pool between storm events. We introduced a holding pool for Agro-IBIS soil leachate and introduced all accumulated mass of nitrate from this holding pool to the wetlands at each runoff event.

Nitrate in groundwater

Nitrate leachate that infiltrates below the rooting zone of croplands is detained to account for travel through the vadose zone and shallow groundwater. WBM does not account for travel through the vadose zone, and only accounts for the hydrodynamic response of the shallow groundwater pool. This temporary detention pool delays transport to approximate the solute travel-time through subsurface flowpaths using an exponential decay weighting function (81–83) given by Eq. 9, which effectively convolves the daily leachate from the soil through a filter of exponential decay:

$$\dot{m}_{rech}^{t} = [1 - \exp(\alpha_{sub}\,dt)]\,\dot{m}_{leach} + \exp(-\alpha_{sub}\,dt)\,\dot{m}_{rech}^{t-1} \quad (9)$$

We assume α_{sub} equal to 0.00125 d^{-1} to capture transit time of solutes through typical catchments (84, 85). DIN experiences denitrification in the subsurface prior to discharge. A constant Dämkoholer number of 0.29 is assumed for the subsurface (86) equating to 25% denitrification of DIN in this pool during transit.

A fraction of all leachate percolating to groundwater (χ_{lost}) is removed from the surface flow system to long-term detention. This accounts for the long-term net storage variable in the subsurface. Without this term, there was a high bias in watershed scale nitrate flux exported at USGS gages. The parameter was calibrated to minimize the bias to observed riverine nitrate flux.

Calibration and corroboration with observations

We corrected bias in riverine flux by calibrating a parameter that directed a portion of percolating nitrate to long-term storage (χ_{lost}), then corroborated the total flux to long-term storage against independent estimates. We compared discharge and nitrate flux at 14 USGS gaging stations throughout the MRB following their selection described in the supplementary material. USGS data were collected through the National Water Inventory System (87), for 44 gaging stations with greater than 200 nitrate samples collected since 1980 at colocated continuous discharge measurements. Monthly flux data are calculated using LOADEST (88) for each station using automated search for the best regression model and linear approximations for the SE. We compared model performance to 14 representative stations where LOADEST succeeded and selected to maintain even spatial sampling across the basin's subwatersheds (see supplementary material). We compared the model with daily discharge and nitrate flux at each station, and summarized model behavior for quarterly and long-term mean values across the entire pool of stations using percent bias (PBIAS), model percent error, Nash–Sutcliffe Efficiency (89), and Kling–Gupta Efficiency (KGE) (90) (Fig. S1). Manual calibration of χ_{lost} on the maximized KGE across the basin resulted in a slight negative bias in simulated monthly nitrate flux (Fig. S1). Monthly simulation of nitrate flux on the Mississippi River at Baton Rouge (Fig. S2) for the unrestored scenario showed a small low-model bias but captured the seasonality of observed fluxes. Our calibrated fluxes of net storage in subsurface storage pools (the vadose zone or groundwater) are within estimates of increased storage below the root zone (32, 51) and to change in groundwater storage owing to increased nitrate concentration (52). Variability in model performance in subcatchments of the basin was not correlated with key geographic inputs. Overestimates of riverine nitrate flux at stations in the western and southern portions of the watershed that were not included in the calibration set of stations suggest a higher fraction of nitrate is stored in deep groundwater in those areas than the model simulated because we selected a parsimonious uniform parameterization across the basin that captures mean basin response.

Datasets used and experimental design

Areas for wetland restoration were selected from existing crops using the Potentially Restorable Wetlands on Agricultural lands (PRW-Ag) dataset (39) selecting any areas identified as either moderate or high potential for restoration. The maximum area for restoration via the Wetland Reserve Program (WRP) was limited to PRW-Ag areas with upstream rainfed crop area equal to 8.4 times the restored area; WRP wetlands (with buffers) were therefore assumed to consist of 12% of their catchment area, consistent with mean wetland/catchment area ratios for natural wetlands in the basin (19, 47). The maximum area for restoration via the FWP was further limited to tile-drained PRW-Ag areas with upstream tile-drained rainfed crop area equal to 22 times the restored area; therefore, FWP wetlands (with buffers) were assumed to consist of 4.5% of their catchments (23). At subpixel scales, we assume that tile-drained lands and rainfed crops are preferentially located on potentially restorable wetland areas. We assume that both wetland program restoration schemas would focus on rainfed crops, as we assume irrigated crop areas to be poorly suited to maintaining levels of inundation needed for wetland restoration. Furthermore, because the PRW-Ag data correlates with tile-drained lands at county and coarser scales (39), we assume the extrapolation of restorable wetlands to be located on tile-drained lands at subpixel scales is also appropriate. We created scenarios of adoption where each pixel was independently increased between the unrestored baseline and its maximum potential restored landcover at 0, 5, 20, 45, 70, and 100% adoption of each program.

Acknowledgments

The authors acknowledge the technical assistance of Alex Prusevich and Stanley Glidden for data and model maintenance. The authors appreciate the feedback on an early draft of this manuscript from Anne Lightbody, J. Matthew Davis, and Mark Green.

Supplementary Material

Supplementary material is available at *PNAS Nexus* online.

Funding

Funding for this research was provided by the National Science Foundation Innovations at the Nexus of Food, Energy, and

Water Systems program Project Grants 1855937 and 1855996. Partial funding was provided by the New Hampshire Agricultural Experiment Station through the USDA National Institute of Food and Agriculture (Hatch, Project Number: 0225006, Scientific Contribution Number: 3011).

Author Contributions

S.Z.—designed and performed research, contributed analytic tools, analyzed data, and wrote the paper. W.M.W. and C.J.K.—designed research, analyzed data, and wrote the paper. R.B.L.—contributed analytic tools and wrote the paper.

Preprints

This manuscript was posted on a preprint: http://dx.doi.org/10.21203/rs.3.rs-2386822/v1.

Data Availability

Data of all self-documented model simulation results are freely available on MyGeoHub (91).

References

1 Diaz RJ, Rosenberg R. 2008. Spreading dead zones and consequences for marine ecosystems. *Science*. 321:926–929.
2 Fennel K, Laurent A. 2018. N and P as ultimate and proximate limiting nutrients in the northern Gulf of Mexico: implications for hypoxia reduction strategies. *Biogeosciences*. 15:3121–3131.
3 Goolsby DA, Battaglin WA, Aulenbach BT, Hooper RP. 2000. Nitrogen flux and sources in the Mississippi River Basin. *Sci Total Environ*. 248:75–86.
4 Tian H, *et al.* 2020. Long-term trajectory of nitrogen loading and delivery from Mississippi River Basin to the Gulf of Mexico. *Global Biogeochem Cycles*. 34:e2019GB006475.
5 Breitburg D, *et al.* 2018. Declining oxygen in the global ocean and coastal waters. *Science*. 359:eaam7240.
6 Dale V. 2010. *Hypoxia in the northern Gulf of Mexico*. New York (NY): Springer Verlag.
7 Scavia D, *et al.* 2017. Ensemble modeling informs hypoxia management in the northern Gulf of Mexico. *Proc Natl Acad Sci U S A*. 114:8823–8828.
8 Marshall E, *et al.* 2018. *Reducing nutrient losses from cropland in the Mississippi/Atchafalaya River Basin: cost efficiency and regional distribution*. Washington (DC): Economic Research Service, US Department of Agiculture.
9 Roy ED, Hammond Wagner CR, Niles MT. 2021. Hot spots of opportunity for improved cropland nitrogen management across the United States. *Environ Res Lett*. 16:035004 .
10 Christianson R, *et al.* 2018. Beyond the nutrient strategies: common ground to accelerate agricultural water quality improvement in the upper Midwest. *J Environ Manage*. 206:1072–1080.
11 Hansen AT, *et al.* 2021. Integrated assessment modeling reveals near-channel management as cost-effective to improve water quality in agricultural watersheds. *Proc Natl Acad Sci U S A*. 118: e2024912118.
12 Liu J, *et al.* 2018. Evaluating alternative options for managing nitrogen losses from corn production. Purdue Policy Research Institute Policy Briefs 4, p. 5.
13 Ribaudo MO, Heimlich R, Claassen R, Peters M. 2001. Least-cost management of nonpoint source pollution: source reduction versus interception strategies for controlling nitrogen loss in the Mississippi Basin. *Ecol Econ*. 37:183–197.
14 Santhi C, *et al.* 2014. An integrated modeling approach for estimating the water quality benefits of conservation practices at the river basin scale. *J Environ Qual*. 43:177–198.
15 Zimmerman EK, Tyndall JC, Schulte LA. 2019. Using spatially targeted conservation to evaluate nitrogen reduction and economic opportunities for best management practice placement in agricultural landscapes. *Environ Manage*. 64:313–328.
16 Jaynes DB, Kaspar TC, Moorman TB, Parkin TB. 2008. In situ bioreactors and deep drain-pipe installation to reduce nitrate losses in artificially drained fields. *J Environ Qual*. 37:429–436.
17 Schipper LA, Robertson WD, Gold AJ, Jaynes DB, Cameron SC. 2010. Denitrifying bioreactors—an approach for reducing nitrate loads to receiving waters. *Ecol Eng*. 36:1532–1543.
18 Jaynes DB, Isenhart TM. 2014. Reconnecting tile drainage to riparian buffer hydrology for enhanced nitrate removal. *J Environ Qual*. 43:631–638.
19 Cheng FY, Van Meter KJ, Byrnes DK, Basu NB. 2020. Maximizing US nitrate removal through wetland protection and restoration. *Nature*. 588:625–630.
20 Mitsch WJ, *et al.* 2001. Reducing nitrogen loading to the Gulf of Mexico from the Mississippi river basin: strategies to counter a persistent ecological ProblemEcotechnology—the use of natural ecosystems to solve environmental problems—should be a part of efforts to shrink the zone of hypoxia in the Gulf of Mexico. *BioScience*. 51:373–388.
21 Christianson L, Tyndall J, Helmers M. 2013. Financial comparison of seven nitrate reduction strategies for Midwestern agricultural drainage. *Water Resour Econ*. 2–3:30–56.
22 Hansen AT, Dolph CL, Foufoula-Georgiou E, Finlay JC. 2018. Contribution of wetlands to nitrate removal at the watershed scale. *Nature Geosci*. 11:127–132.
23 Iovanna R, Hyberg S, Crumpton W. 2008. Treatment wetlands: cost-effective practice for intercepting nitrate before it reaches and adversely impacts surface waters. *J Soil Water Conserv*. 63: 14A–15A.
24 Zou J, *et al.* 2022. Rewetting global wetlands effectively reduces major greenhouse gas emissions. *Nat Geosci*. 15:627–632.
25 Mitchell ME, *et al.* 2022. Potential of water quality wetlands to mitigate habitat losses from agricultural drainage modernization. *Sci Total Environ*. 838:156358.
26 Czuba JA, Hansen AT, Foufoula-Georgiou E, Finlay JC. 2018. Contextualizing wetlands within a river network to assess nitrate removal and inform watershed management. *Water Resour Res*. 54:1312–1337.
27 Carleton JN, Montas HJ. 2010. An analysis of performance models for free water surface wetlands. *Water Res*. 44:3595–3606.
28 Lightbody AF, Avener ME, Nepf HM. 2008. Observations of short-circuiting flow paths within a free-surface wetland in Augusta, Georgia, USA. *Limnol Oceanogr*. 53:1040–1053.
29 Crumpton WG, Stenback GA, Fisher SW, Stenback JZ, Green DIS. 2020. Water quality performance of wetlands receiving nonpoint-source nitrogen loads: nitrate and total nitrogen removal efficiency and controlling factors. *J Environ Quality*. 49: 735–744.
30 Baker BH, *et al.* 2018. Nutrient and sediment runoff from agricultural landscapes with varying suites of conservation practices in the Mississippi Alluvial Valley. *J Soil Water Conserv*. 73:75–85.
31 Fisher J, Acreman MC. 2004. Wetland nutrient removal: a review of the evidence. *Hydrol Earth Syst Sci*. 8:673–685.

32 Van Meter KJ, Basu NB, Veenstra JJ, Burras CL. 2016. The nitrogen legacy: emerging evidence of nitrogen accumulation in anthropogenic landscapes. *Environ Res Lett*. 11:035014.

33 Van Meter KJ, Van Cappellen P, Basu NB. 2018. Legacy nitrogen may prevent achievement of water quality goals in the Gulf of Mexico. *Science*. 360:427–430.

34 Carstensen MV, *et al*. 2020. Efficiency of mitigation measures targeting nutrient losses from agricultural drainage systems: a review. *Ambio*. 49:1820–1837.

35 Rajib A, Golden HE, Lane CR, Wu Q. 2020. Surface depression and wetland water storage improves major river basin hydrologic predictions. *Water Resour Res*. 56:e2019WR026561.

36 Valayamkunnath P, Barlage M, Chen F, Gochis DJ, Franz KJ. 2020. Mapping of 30-meter resolution tile-drained croplands using a geospatial modeling approach. *Sci Data*. 7:257.

37 Sugg Z. 2007. *Assessing U.S. Farm drainage: can GIS lead to better estimates of subsurface drainage extent?*. Washington (DC): World Resources Institute.

38 Evenson GR, *et al*. 2021. Wetland restoration yields dynamic nitrate responses across the upper Mississippi River Basin. *Environ Res Commun*. 3:095002.

39 Horvath EK, Christensen JR, Mehaffey MH, Neale AC. 2017. Building a potential wetland restoration indicator for the contiguous United States. *Ecol Indic*. 83:462–473.

40 Natural Resources Conservation Service. 2010. Wetland restoration (Ac.). In: *National handbook of conservation practices*. Washington (DC): US Department of Agriculture. p. 5.

41 Kucharik CJ. 2003. Evaluation of a process-based agro-ecosystem model (Agro-IBIS) across the U.S. Corn belt: simulations of the interannual variability in maize yield. *Earth Interact*. 7:1–33.

42 Kucharik CJ, Brye KR. 2003. Integrated Biosphere simulator (IBIS) yield and nitrate loss predictions for Wisconsin maize receiving varied amounts of nitrogen fertilizer. *J Environ Qual*. 32:247–268.

43 Donner SD, Kucharik CJ. 2008. Corn-based ethanol production compromises goal of reducing nitrogen export by the Mississippi River. *Proc Natl Acad Sci U S A*. 105:4513–4518

44 Stewart RJ, *et al*. 2011. Separation of river network–scale nitrogen removal among the main channel and two transient storage compartments. *Water Resour Res*. 47(10):W00J10.

45 Samal NR, *et al*. 2017. A coupled terrestrial and aquatic biogeophysical model of the Upper Merrimack River watershed, New Hampshire, to inform ecosystem services evaluation and management under climate and land-cover change. *Ecol Soc*. 22:18.

46 Grogan DS, *et al*. 2022. Water balance model (WBM) v.1.0.0: a scalable gridded global hydrologic model with water-tracking functionality. *Geosci Model Dev*. 15:7287–7323.

47 Wu Q, Lane CR. 2017. Delineating wetland catchments and modeling hydrologic connectivity using lidar data and aerial imagery. *Hydrol Earth Syst Sci*. 21:3579–3595.

48 Mitsch WJ, Day JW. 2006. Restoration of wetlands in the Mississippi–Ohio–Missouri (MOM) river basin: experience and needed research. *Ecol Eng*. 26:55–69.

49 Wollheim W, *et al*. 2014. Nitrate uptake dynamics of surface transient storage in stream channels and fluvial wetlands. *Biogeochemistry*. 120:239–257.

50 Green CT, *et al*. 2008. Limited occurrence of denitrification in four shallow aquifers in agricultural areas of the United States. *J Environ Qual*. 37(3):994–1009.

51 Ascott MJ, *et al*. 2017. Global patterns of nitrate storage in the vadose zone. *Nat Commun*. 8:1416.

52 Puckett LJ, Tesoriero AJ, Dubrovsky NM. 2011. Nitrogen contamination of surficial aquifers—a growing legacy. *Environ Sci Technol*. 45:839–844.

53 Dupas R, Ehrhardt S, Musolff A, Fovet O, Durand P. 2020. Long-term nitrogen retention and transit time distribution in agricultural catchments in western France. *Environ Res Lett*. 15:115011.

54 Cheng FY, Basu NB. 2017. Biogeochemical hotspots: role of small water bodies in landscape nutrient processing. *Water Resour Res*. 53:5038–5056.

55 Tanner CC, Sukias JPS, Yates CR. 2010. *Constructed wetland treatment of tile drainage*. Hamilton: National Institute of Water & Atmospheric Research Ltd.

56 Mulholland PJ, *et al*. 2008. Stream denitrification across biomes and its response to anthropogenic nitrate loading. *Nature*. 452:202–205.

57 Racchetti E, *et al*. 2011. Influence of hydrological connectivity of riverine wetlands on nitrogen removal via denitrification. *Biogeochemistry*. 103:335–354.

58 Bachand PA, Horne AJ. 1999. Denitrification in constructed free-water surface wetlands: I. Very high nitrate removal rates in a macrocosm study. *Ecol Eng*. 14:9–15.

59 Basu NB, *et al*. 2022. Managing nitrogen legacies to accelerate water quality improvement. *Nat Geosci*. 15:97–105.

60 Scott DT, Keim RF, Edwards BL, Jones CN, Kroes DE. 2014. Floodplain biogeochemical processing of floodwaters in the Atchafalaya River Basin during the Mississippi River flood of 2011. *J Geophys Res Biogeosci*. 119:537–546.

61 Gourevitch JD, *et al*. 2020. Spatial targeting of floodplain restoration to equitably mitigate flood risk. *Glob Environ Change*. 61:102050.

62 Conservation Reserve Program. 2015. *Farmable wetlands program, constructed wetlands*. Washington (DC): USDA Farm Service Agency.

63 Kucharik CJ, *et al*. 2000. Testing the performance of a dynamic global ecosystem model: water balance, carbon balance, and vegetation structure. *Global Biogeochem Cycles*. 14:795–825.

64 Donner SD, Kucharik CJ. 2003. Evaluating the impacts of land management and climate variability on crop production and nitrate export across the Upper Mississippi Basin. *Global Biogeochem Cycles*. 17:1085.

65 Ferin KM, *et al*. 2021. Water quality effects of economically viable land use change in the Mississippi river basin under the renewable fuel standard. *Environ Sci Technol*. 55:1566–1575.

66 Ramankutty N, Evan AT, Monfreda C, Foley JA. 2008. Farming the planet: 1. Geographic distribution of global agricultural lands in the year 2000. *Global Biogeochem Cycles*. 22:GB1003

67 Siebert S, Döll P. 2010. Quantifying blue and green virtual water contents in global crop production as well as potential production losses without irrigation. *J Hydrol (Amst)*. 384:198–217.

68 Han W, Yang Z, Di L, Mueller R. 2012. CropScape: a web service based application for exploring and disseminating US conterminous geospatial cropland data products for decision support. *Comput Electron Agric*. 84:111–123.

69 Wollheim W, Peterson BJ, Thomas SM, Hopkinson CS, Vorosmarty CJ. 2008. Dynamics of N removal over annual time periods in a suburban river network. *J Geophys Res Biogeosci*. 113:G03038.

70 Zuidema S. 2022. *Interventions towards sustainable watershed management as demonstrated by hydrologic simulation*. Durham (NH): University of New Hampshire.

71 Eilander D, *et al*. 2021. A hydrography upscaling method for scale-invariant parametrization of distributed hydrological models. *Hydrol Earth Syst Sci*. 25:5287–5313.

72 Kadlec RH, Knight RL. 1996. *Treatment wetlands*. Boca Raton (FL): CRC Press.

73 Martinez CJ, Wise WR. 2003. Hydraulic analysis of Orlando easterly wetland. *J Environ Eng*. 129:553–560.
74 Carleton JN. 2002. Damköhler number distributions and constituent removal in treatment wetlands. *Ecol Eng*. 19:233–248.
75 Kjellin J, Wörman A, Johansson H, Lindahl A. 2007. Controlling factors for water residence time and flow patterns in Ekeby treatment wetland, Sweden. *Adv Water Resour*. 30:838–850.
76 Groffman PM, Gold AJ, Addy K. 2000. Nitrous oxide production in riparian zones and its importance to national emission inventories. *Chemosphere Global Change Science*. 2:291–299.
77 Lutz SR, *et al*. 2020. How important is denitrification in riparian zones? Combining end-member mixing and isotope modeling to quantify nitrate removal from riparian groundwater. *Water Resour Res*. 56:e2019WR025528.
78 Mayer PM, Reynolds SK, McCutchen MD, Canfield TJ. 2007. Meta-analysis of nitrogen removal in riparian buffers. *J Environ Qual*. 36:1172–1180.
79 Kadlec RH, Reddy KR. 2001. Temperature effects in treatment wetlands. *Water Environ Res*. 73:543–557.
80 Wollheim W, Vorosmarty CJ, Peterson BJ, Seitzinger SP, Hopkinson CS. 2006. Relationship between river size and nutrient removal. *Geophys Res Lett*. 33:L06410.
81 Sangrey DA, Harrop-Williams KO, Klaiber JA. 1984. Predicting ground-water response to precipitation. *J Geotech Eng*. 110: 957–975.
82 Venetis C. 1969. A study on the recession of unconfined acquifers. International association of scientific hydrology. *Bulletin*. 14:119–125.
83 Neitsch SL, Arnold JG, Kiniry JR, Williams JR. 2011. *Soil and water assessment tool theoretical documentation version 2009*. College Station (TX): Texas Water Resources Institute.
84 Benettin P, *et al*. 2015. Linking water age and solute dynamics in streamflow at the Hubbard Brook Experimental Forest, NH, USA. *Water Resour Res*. 51:9256–9272.
85 Berghuijs WR, Kirchner JW. 2017. The relationship between contrasting ages of groundwater and streamflow. *Geophys Res Lett*. 44:8925–8935.
86 Green CT, *et al*. 2008. Limited occurrence of denitrification in four shallow aquifers in agricultural areas of the United States. *J Environ Qual*. 37:994–1009.
87 U.S. Geological Survey. 2001. National Water Information System data available on the World Wide Web (Water Data for the Nation) at https://waterdata.usgs.gov/dc/nwis/doc?citation_help.
88 Runkel RL, Crawford CG, Cohn TA. 2004. *Load estimator (LOADEST): a FORTRAN program for estimating constituent loads in streams and rivers. Techniques and methods book 4, Chapter A5*. Reston (VA): US Geological Survey. p. 1–75.
89 Nash JE, Sutcliffe JV. 1970. River flow forecasting through conceptual models part I–A discussion of principles. *J Hydrol (Amst)*. 10:282–290.
90 Gupta HV, Kling H, Yilmaz KK, Martinez GF. 2009. Decomposition of the mean squared error and NSE performance criteria: implications for improving hydrological modelling. *J Hydrol (Amst)*. 377:80–91.
91 Zuidema S, Kucharik CJ, Lammers RB, Wollheim WM. 2022. Data: Existing wetland conservation programs miss nutrient reduction targets. MyGeoHub. https://doi.org/10.13019/1N4Q-0X09.